COMPREHENSIVE AND STANDARDIZED BENCHMARKING OF DEEP LEARNING ARCHITECTURES FOR BASECALLING NANOPORE SEQUENCING DATA

Marc Pagès-Gallego
Center for Molecular Medicine
University Medical Center Utrecht
Universiteitsweg 100, 3584 CG Utrecht
m.pagesgallego@umcutrecht.nl

Jeroen de Ridder
Center for Molecular Medicine
University Medical Center Utrecht
Universiteitsweg 100, 3584 CG Utrecht
j.deridder-4@umcutrecht.nl

May 17, 2022

ABSTRACT

Nanopore basecalling is a difficult task which requires the use of complex algorithms and neural network models to achieve competitive accuracies. These algorithms, called basecallers, are developed continuously both by ONT and the scientific community in an effort to improve basecalling accuracies. With the rapidly increasing number of basecallers, the need for thorough benchmarking and comparison of basecallers grows. However, benchmarking is currently not standardized, and evaluation metrics and datasets used are defined on a per publication basis. This makes it difficult to compare models and to differentiate between algorithm or data driven improvements. In an effort to standardize the process of benchmarking, we unified existing benchmarking datasets to propose a set of training and testing challenges. We also defined a wide array of evaluation metrics to test the strengths and weaknesses of the models. Given these data challenges and evaluation metrics, we benchmarked the latest seven basecaller models as well and analyzed their architectures by combining their different neural network components.

Keywords Nanopore · Basecalling · Deep learning · Benchmark

1 Introduction

Sequencing of DNA (or RNA) can be achieved by translocating nucleic acids in an ionic flow through a nanopore via a motor protein. By passing an electric current through the nanopore, a signal is measured that is representative for the chemical nature of the different nucleotides inside the pore. Therefore, capturing this current yields a signal that can be translated into a DNA sequence. In 2014, Oxford Nanopore Technologies (ONT) released the first commercial sequencing devices based on this principle. Compared to other sequencing technologies, nanopore sequencing offers several advantages. For instance, unlike short-read sequencing platforms, nanopore sequencing does not have a fundamental limitation on the read length, allowing the correct mapping of highly repetitive regions [1] and facilitating structural variant calling [2]. Moreover, the translation of the electric signal to DNA sequence can occur in real time, dramatically shortening the time between sample collection and data analysis, having the potential to be applied for time-critical clinical diagnostics [3]. Finally, base modifications such as 5-methylcytosine or 6-methyladenosine give rise to distinct changes in the signal, providing the opportunity to directly sequence DNA modifications [4].

One of the fundamental steps in nanopore sequencing is the process of translating the raw current signal to a DNA sequence [5], because almost all downstream applications depend on it [6]. This step, called basecalling, is far from trivial due to several reasons. First of all, the current signal is most dominantly influenced by the several nucleotides that reside inside the pore at any given time. For example, 5-6 nucleotides influence the signal in R9.4 pores. As a result, in an idealized situation, and under the assumption that the DNA consists of only four canonical bases, there can be 4^5 signal states that have to be distinguished. Because of noise in the signal that results from fluctuations in the

ion flow in the pore, it is not always possible to reliably match the measured current signal to the correct 5-mer state. Moreover, the number of unique signal states increases polynomially for each additional base, such as bases modified by methylation. A second complicating factor is that DNA molecules do not move through the nanopore at a constant speed. Therefore, the number of signal measurements is not a good estimate on the corresponding number of bases. Instead, the detection of changes in the signal is required to determine that the next base has entered the pore. This is problematic for stretches of single-base repeats (homopolymers), where the signal remains constant, and indeed nanopore sequencing suffers from increased error rates in this situation.

To address this challenge, a wide array of basecallers has been developed both by ONT and the wider scientific community. The first generation of basecallers relied on segmenting the signal base by base, and then applying simple statistics describing the expected signal levels per k-mer. Subsequently, Hidden Markov Models (HMMs) made their introduction that better leveraged temporal dependencies in the signal. The first introduction of neural networks for this task was in *DeepNano* [7], which was used to classify the signal segments. *BasecRAWler* [8] used two independent neural networks to first segment the signal, and then classify the segments. Finally, *Chiron* [9] used a single end-to-end neural network to skip the segmentation step altogether. After 2018, and thanks to their rise in popularity in other fields, neural networks have been the go-to machine learning algorithm for basecalling because of their flexibility, speed and performance despite their high requirements of training data and large number of tunable hyperparameters.

Wick et al. (2019) benchmarked *Chiron* and four other ONT basecallers that were being developed at the time: *Albacore*, *Guppy*, *Scrappie* and *Flappie*. *Chiron* used developments in the speech to text translation field as it applied a Convolutional Neural Network (CNN) to extract the features from the raw signal, a Recurrent Neural Network (RNN) to relate such features in a temporal manner, and a Connectionist Temporal Classification (CTC) decoder [10] to avoid segmenting the signal. Since then, many other basecallers have been developed and published by the community (Figure 1): *Mincall* [11] used a deep CNN with residual connections [12], *Causalcall* [13] used a CNN with causal dilatations [14], *SACall* [15] and *CATCaller* [16] used transformers [17] and lite-transformers [18] respectively, *URNano* [19] used a convolutional U-net with integrated RNNs [20], and *Halcyon* [21] used a sequence-to-sequence (Seq2Seq) model with attention [22, 23]. ONT also updated its main basecaller (*Guppy*) with the *Bonito* architecture, which substituted the CTC decoder with a conditional random field (CRF) decoder [24].

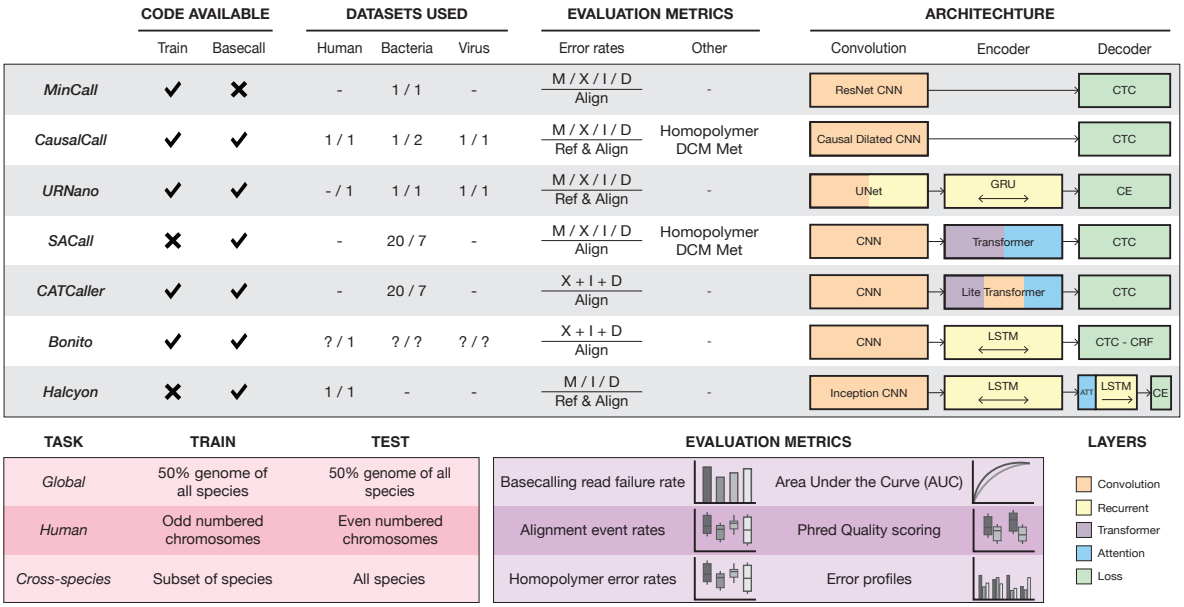

Figure 1: Overview of the latest basecaller models and benchmark. Code available columns indicate whether their github repositories contained scripts to train a model from scratch or basecall using their trained models. Values in the datasets indicate the number of species they used for training (left) and testing (right). Alignment rates reported for: matches (M), mismatches (X), insertions (I) and deletions (D); and whether they were normalized based on the length reference sequence (Ref) or the length of the alignment (Align). Metrics separated by a slash (/) are reported independently, others are reported as a combined error rate. Some models also report homopolymer and methylation site error rates. The architecture section shows a high level overview of the different models. Overview of the different tasks in the benchmark with their respective training and testing data (pink). Overview of the evaluation metrics in the benchmark (purple).

Collectively, all these models have pushed basecalling accuracy from approximately 89% in 2019 to >95% in 2022. It is reasonable to assume that, with new AI methods being continuously developed and tailored to various applications, more improvements are around the corner. Problematically, currently no standardized benchmarking methods, training and evaluation datasets or performance metrics for basecalling exist [5]. For new basecalling algorithms, evaluation metrics are often defined on a per-publication basis and are limited to only certain aspects of basecalling accuracy, such as single base errors ignoring indel error. This may bias conclusions as more favorable metrics are chosen for head to head algorithm comparisons. Furthermore, data used for training and testing is not uniform across publications, which makes it difficult to distinguish between data or neural network architecture driven improvements. Leading to progress impediments in the field and precludes easy comparison of published algorithms and results (Figure 1). This is in stark contrast to e.g., the field of machine learning itself, where new models and methods are benchmarked with community driven evaluation metrics and datasets, such as the CASP competition [25] and the CAMI benchmark [26]. Such efforts facilitate the comparison of new and existing models, and the identification of their respective strengths and weaknesses [27]. It also centralizes all the information, making it easier for users to find the best method for their end goal and lowering the bar to take on the challenge for new developers.

Here we present a wide set of evaluation metrics that can be used to analyze the strengths and weaknesses of basecaller models. This toolbox can be used as benchmark for the standardized training and cross-comparison of existing and future basecallers. Using this toolbox we benchmarked the latest basecaller models. We also created and benchmarked over eighty novel neural network architectures by combining the different components of existing basecaller models. This allowed us to study the effect on performance of the different neural networks components, as well as explore potentially better performing architectures. Finally, we also benchmarked the top performing architectures using different training and testing datasets; allowing us to we evaluate the robustness of the models to the training data and its driving force in model performance. Together, our work provides insight into what the best model architecture is under what conditions and establishes that model architectures not currently implemented in existing basecalling tools outperform state of the art for certain metrics.

2 Results

2.1 Benchmark setup

We first developed a basecalling benchmarking framework enabling new and existing basecalling algorithms to be easily compared. Moreover, our benchmark facilitates the study of individual components of basecallers, as different combinations of basecaller components can readily be evaluated. The framework is divided into two main components: (i) standardized datasets for model training and evaluation addressing different real-world basecalling tasks and (ii) evaluation metrics for extensive assessment of basecalling performance (Figure 1). This setup enables keeping the datasets and evaluation metrics fixed to ensure that differences in performance are due to method differences and allow detailed study of what aspect of the performance changes depending on neural network architecture. For instance, it is possible to determine that a certain architecture is better at calling indels while another excels in reducing homopolymer errors. The benchmark components are fully automated with minimal dependencies and publicly available at github , making it easy for developers to focus on algorithm development.

Datasets and tasks We gathered datasets that have previously been used for benchmarking, were available for download and were sequenced using the R9.4 or R9.4.1 pore chemistry. This yielded 615642 reads from 3 human datasets, 1 Lambda phage dataset and 60 bacterial datasets encompassing 26 different bacterial species. After read annotation using *tombo*, 460225 reads (75%) were suitable for benchmarking (Supplemental figure 1; Supplementary Table 1). Because Nanopore sequencing has several possible downstream applications, we aimed to include datasets to address different real world use-case scenarios, enabling assessment of which basecaller is better suited for a certain task. To this end, we define three different tasks: global, human and cross-species that each use specific portions of training and test data (Supplementary Table 1).

The global task evaluates the performance of a general-purpose model by training and testing the model using data from all available species. In this task, models have access to most data, which is a similar strategy employed in *Causalcall* and *URNano*. The human task evaluates the performance of a human specialized model by training and testing exclusively on human data. To our knowledge, species specialized models are not currently being applied. However, this strategy is used in *Halcyon* and *Mincall*, although in the latter model *E. coli* is used as species. While here we only define this task for human data, a similar task can be defined to test specialization to other species. The cross-species task evaluates the performance of a trained model on never before seen species. This allows us to evaluate the ability of the model to not overfit on the specific k-mer composition within the training data. This is achieved by training using a subset of bacterial species and testing on data from all species. This is most similar to the benchmark by Wick et al., (2019) and similar to the evaluation strategy followed in *SACall* and *CATCaller* models. However, here

we explicitly take into account the similarity in their genome k-mer composition when splitting species between train and test sets to define test datasets of varying difficulty (see Methods).

Evaluation metrics We define six basecalling evaluation metrics allowing making unbiased and quantitative comparisons of basecalling efficacy across various conditions.

- **Basecalling read failure rate:** not all reads can be successfully basecalled. Failed reads are excluded from any subsequent evaluation. It is therefore important to report the failure rate of the model. Read basecalling failure falls into one of several categories: not basecalled (the model did not produce any basecalls), not aligned (during evaluation, the alignment algorithm did not produce an alignment), short alignment (the length of the alignment is less than 50% of the length of the reference), or other (other possible errors that prevent the read from being evaluated).
- **Alignment rates:** after alignment of a basecalled read to its reference, four types of events can be distinguished: matches, mismatches, insertions and deletions. It is important to report the different types of events independently, since two models may have similar match rates but have different profiles in the types of errors they produce. Event rates, for all four cases, are calculated by counting the number of each event type and dividing them by the length of the alignment for each read.
- **Homopolymer error rates:** homopolymers are particularly difficult to basecall in Nanopore sequencing. For this reason, an independent metric is used to report them. Homopolymers are defined by any repetitive sequence of the same base of length 5 or longer. Homopolymer error rates are calculated by dividing the number of errors in homopolymers by the total number of homopolymer bases for each base independently.
- **Error profiles:** basecalling errors can have different distributions depending on the bases that surround the event. Similar to the trinucleotide context used to define mutational signatures [28], we can subdivide the errors based on its sequence context to study potential sequence bias in the errors. Ideally, a model's error profile is unbiased and uniform, for example, to avoid biased variant calling. Error profiles are calculated by counting the number of events of the middle base for each 3-mer and dividing them by the total amount of basecalled 3-mers. Mismatches are further subdivided for each type of mismatch.
- **Phred Quality (PhredQ) scoring:** PhredQ scores are values that indicate the confidence of the model in its prediction of a base. Ideally, potential incorrect calls have low quality scores while high scoring bases are mostly correct. PhredQ scores can be calculated from the predicted distribution of probabilities. However, because of the difference in the number of possible outcomes between decoder types (CTC, CRF, or Seq2Seq), the calculation of the PhredQ score varies. We therefore rely on the PhredQ scores as specified by the developers of each basecalling method. We report the mean value of PhredQ scores for correct and incorrect bases per read.
- **Area under the Curve (AUC):** PhredQ scores can also be used to evaluate the model at read level. This is done by evaluating the trade-off between filtering out bad quality reads and the change in performance of the model. This is done by sequentially removing the worst 10 reads according to their mean PhredQ score and calculating the average match rate of the remaining fraction of reads.

2.2 Benchmark results

The results of the human benchmarking challenge are summarized in Figure 2 and Supplementary Table 2.

Basecalling failure is a major determinant of reported performance We first note that the number of reads that failed basecalling varies substantially. Distinctively, *Causacall* and *Halcyon* only managed to properly basecall 66% and 79% of the reads, respectively. For *Causalcall* most of the failed reads are reads that do not give a good enough alignment to the reference (25%), followed by reads whose alignment was shorter than 50% of the reference length (7%). For *Halcyon* most of the failures also come from reads with a short alignment to the reference sequence (15%) (Figure 2a). It is therefore critical to include such a metric in model evaluation since for two main reasons: first, models could be skipping difficult to basecall reads, which would skew results towards a false higher performance due to only basecalling easy reads; and second, properly basecalled reads are not different than poorly basecalled reads from the end user perspective, and the latter could hamper downstream analysis.

Different methods prevail at different tasks / measures Secondly, we evaluate the performance of the models using the alignment event rates (Figure 2b). *Bonito* performed best in three out of the four metrics. It has the highest median match rate (90%) and the lowest median mismatch (2.5%) and deletion (4.3%) rates. *Causalcall* achieved the lowest median insertion rate (1.7%); however, it performed worst in the other three metrics with the lowest median match rate

(77.6%) and highest mismatch (6%) and deletion (14.4%) rates. Another distinctive performance is the one of *Halcyon*, as it shows the highest variation in performance per read in match, insertion and deletion rates, demonstrating that, in addition to the median, the distribution across the reads is important to consider while comparing basecallers. The rest of the models showed small differences among them, with maximum rate differences being match (2.8%), mismatch (1.7%), insertion (1.7%) and deletion (2.6%). Our results show that, while *Bonito* is in general the best performer, if low insertion rates are preferred, *Causalcall* would be the best choice, at the cost of increased mismatch and deletion errors.

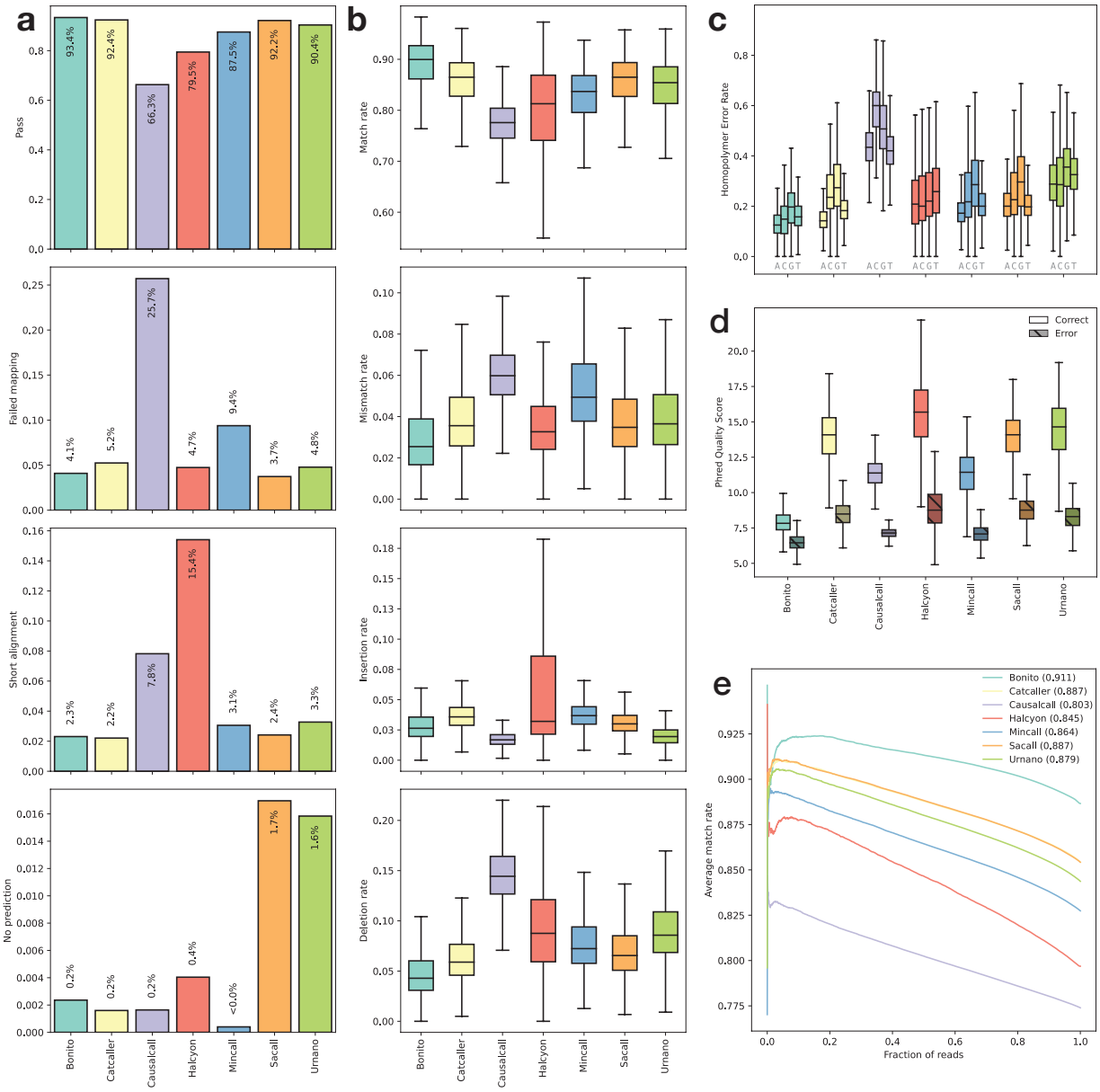

Figure 2: Latest basecallers benchmark on the human task. **(a)** basecalling reads failure rates: pass, failed mapping, short alignment and no prediction (from top top bottom). **(b)** alignment event rates: match, mismatch, insertion and deletion (from top to bottom). **(c)** homopolymer error rates per base. **(d)** PhredQ scores distributions for correctly (light) and incorrectly (dark) predicted bases. **(e)** AUC of match rate sorted by average read PhredQ score.

Homopolymer results are correlated with alignment event rates Thirdly we evaluate the homopolymer error rates (Figure 2c). Homopolymers are especially difficult to basecall because, for long stretches of the same base, the signal does not change, and since the DNA translocation speed is not constant, the number of measurements is not a good

indicator of the length of the homopolymer. *Bonito* performed best with the lowest median error rate (14.9% averaged across all four bases), and moreover has the lowest median error rate for each base individually. *Causalcall* performed significantly worse than the rest of the models with the highest median error rate (44.5% averaged across bases). We observe a performance correlation between alignment event rates and homopolymer error rates; however, the latter have a significantly higher error rate likely due to their difficulty. A general trend across models is that, adenine and thymine homopolymers have lower error rates than cytosine and guanine homopolymers, suggesting some homopolymer bases are easier to basecall than others.

Utility of Phred quality scores varies across methods We next evaluate the relationship between the predicted bases and their phred quality scores. First, we consider the distributions of the scores of the correct and incorrect bases (Figure 2d). For all models, correct bases have higher scores than incorrect bases; *Causalcall* has the smallest overlap between the two distributions (0.7%), followed by the rest of the models with similar overlaps (6-8%) except *Halcyon* (12%) and *Bonito* (32%). Secondly, we calculate AUCs by sorting the reads based on their average quality scores and determining the area under the normalized cumulative score (Figure 2e). All models showed a correlation between read quality and average match rate. Not surprisingly, *Bonito* performed best with an AUC of 0.91. *CATCaller* and *SACAll* are, however, close contenders both with an AUC of 0.886. Most of the remaining models achieved AUCs higher than 0.85. Importantly, despite being calculated in the same way, each model has its own PhredQ score offset that determines how their quality scores are calibrated. As a result, quality scores across models, even when compared in a standardized benchmark, are not directly comparable numerically.

The signatures of basecalling errors Finally, we evaluate the different types of mistakes in the context of the two neighboring bases in the basecalls (Supplementary Figure 2a-g). In general, these error 'signatures' reveal that there are differences between the accuracy of the models depending on the predicted base context. Across all models, cytosine has low error rates (10%) when predicted in CCT or TCT context, however, it can have significantly higher error rates (>30%) when predicted in the context of the 3-mers TCC or TCG. Similar examples can be found for guanine as well: CGC and CGG have higher error rates (>30%) while GGA and GGC have low error rates (10%). Adenine and thymine also have 3-mer context biases, however their differences are not as extreme. To evaluate if specific models have particular error biases we performed hierarchical clustering on the pairwise Jensen-Shannon divergences between the error signatures ((Supplementary Figure 3)). This reveals that *Causalcall* and *Halcyon* are the two most different models in terms of error 'signatures'. From the error signature profiles of the individual models (Supplementary Figure 2c), we find that the elevated deletion errors and reduced insertion errors of *Causalcall* are relatively uniformly distributed across all contexts. In contrast, the errors made by *Halcyon* are more dominant for certain contexts (Supplementary Figure 2d). The rest of the models have similar error profiles (lowest Pearson correlation coefficient between them: 0.95). We can conclude that basecalling errors are biased since they are not uniformly distributed across the 3-mer contexts; however, the error profiles are very similar between basecallers, suggesting that training data may play a stronger role in defining these error biases than the architecture of the model.

Model implementation makes small differences compared to the original models Since *Causalcall* and *Halcyon* performed worse than the rest of the models, we evaluated the original models *Causalcall*, *Halcyon* and *Guppy* model published by the authors, and compared them against our PyTorch implementations (Supplementary Figure 4, Supplementary Table 3). In terms of reads that we consider evaluable, we see small differences (less than 3%) between the original versions and our implementations of *Causalcall* and *Guppy*. However, we see some differences in the types of failed reads between the original *Causalcall*, which has 7% more reads that failed mapping; whereas our recreation had 3% more reads with short alignments. Surprisingly, basecalls from the original *Halcyon* produce only 46% of reads suitable for evaluation, (30% less than our recreation). A significant 34% of reads failed mapping (30% more than our recreation) to the reference. There is also an increase, although smaller, on the 19% of reads that have short alignments to the reference (5% more than our recreation) (Supplementary Figure 4a). Regarding our implementation of *Guppy*, we find that differences are small, with at most a 2% difference. We then looked at the alignment event rates (Supplementary Figure 4b). Differences between the two *Guppy* models were very small, with the largest being a 1.3% difference in increased match rate from the original version. The original *Causalcall* showed improved match performance, with increased match (2%) and a decreased deletion (6%) rates; however it showed a slight increase in mismatch (1%) and insertion (1%) rates as well as higher variability across reads. Finally, the original *Halcyon* performed worse in all metrics except deletion rate. However, its performances are less variable across reads. Homopolymer error rates show a similar trend (Supplementary Figure 4c), the original *Causalcall* performs significantly better with a more similar to the other models average error rate (25.6%) while the other two models show very similar performances. We finally compared the models regarding their PhredQ scores: when comparing *Bonito* to *Guppy* we saw a large difference in the scale of the scores (Supplementary Figure 4d), however, *Guppy* still had an overlap between the distributions of 28%. On the other hand, the original *Causalcall* showed a significant increase in the overlap between distributions (48%). (Supplementary Figure 4e). Correlating with the event rates results, the original versions of *Causalcall* and *Guppy*

performed slightly better than our recreated counterparts with AUCs of 0.837 and 0.937 respectively. The original *Halcyon* does not report any PhredQ scores. With these results, we concluded that although there are some differences between the original models and our recreations, these are minor and could be attributed to training strategies and used data.

2.3 Architecture analysis

The benchmarking setup also allows straightforward investigation of which components of the neural networks provide the main performance gains. To this end, we created novel architectures by combining the convolution, encoder and decoder modules of existing basecallers, as well as some additional modules. We again used the human task to evaluate the different models. In total, ninety different models were evaluated and ranked based on the sum of rankings across all metrics (Figure 3a, Supplementary Figure 5). Out of the original models, *Bonito* again performs best, but only reached 9th place in the overall ranking. Consequently, our grid search reveals eight new model architectures that performe better in general. However, improvements in performance made by these models are small; for example in comparison to the *Bonito* model, the alignment event rate improvements and homopolymer error rates are smaller than 1%, suggesting that we may be reaching the performance limits obtainable given the training data used.

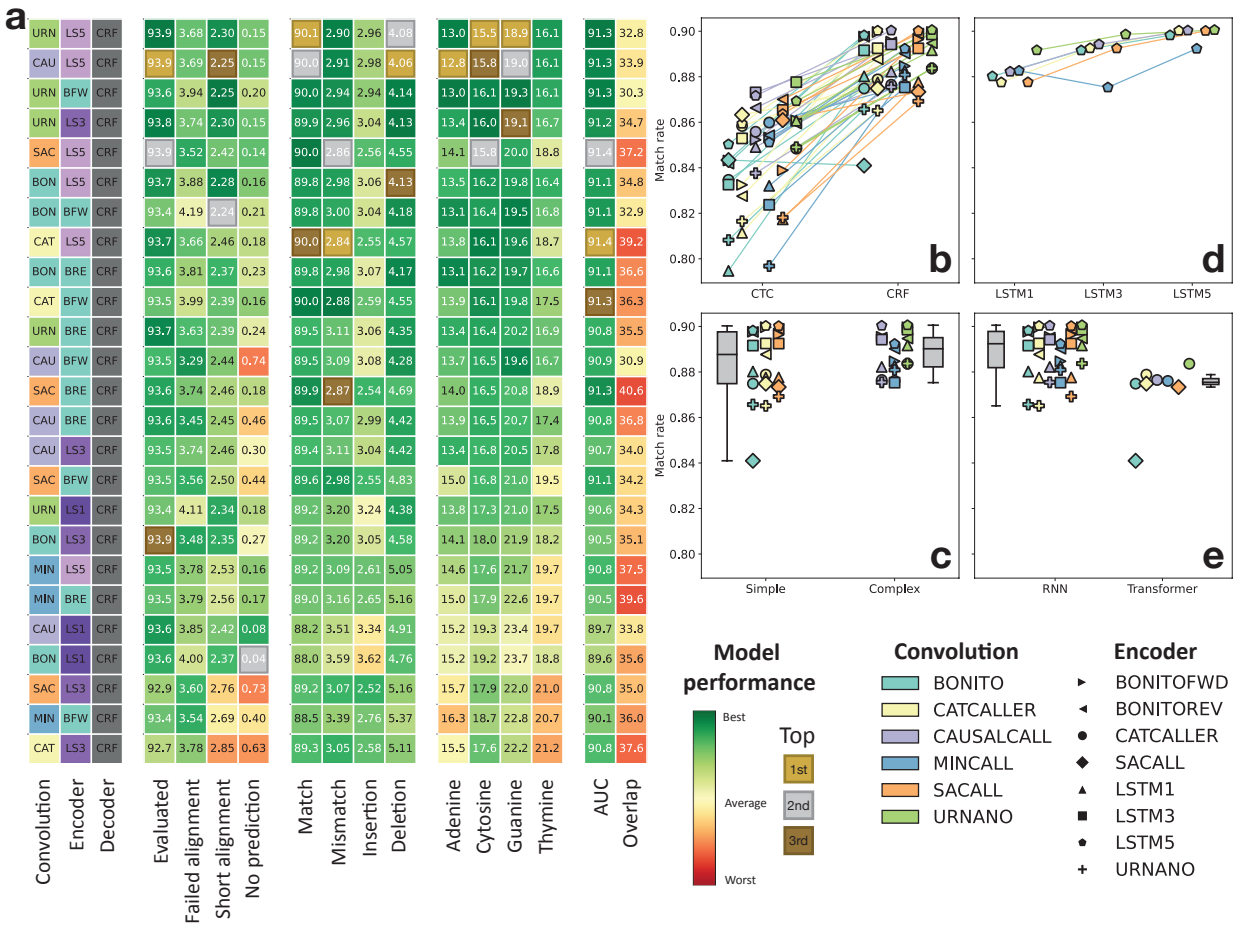

Figure 3: Benchmark of architecture components. (a) Top 25 best performing model combinations. **(b)** Comparison of CTC to CRF decoder. **(c)** Comparison of simple (*Bonito*, *CATCAller*, *SACall*) to complex (*Causalcall*, *Mincall*, *URNano*) convolutions. **(d)** Comparison of bidirection LSTM depth (1, 3 or 5 layers). **(e)** Comparison of RNN to Transformer encoders.

CRF decoder is vastly superior to CTC The architectural grid search enables evaluation of which modules contribute most to the basecalling performance. We observed that most of the high performing models used the CRF decoder

module. We therefore compared the change in performance between pairs of models whose only difference was the decoder (Figure 3b, Supplementary Figure 6). We see that for almost all models, using a CRF decoder leads to a general improvement of performance with a mean increase in match rate of 4% and mean decreases of mismatch, insertion and deletion rates of 1%, 1% and 2% respectively. Some exceptions are models that used the *Mincall* or *URNano* convolution modules, which have a mean increase in insertion rates of 1%; although their other alignment rate metrics still improve significantly. This is in concordance with our previous results, where *Causalcall* and *URNano* demonstrated the lowest insertion rates of all the models, showcasing that it is their convolutional architectures that boosts performance for this type of metric. Notably, a decrease in homopolymer error rates is also observed for the models with *Mincall* or *URNano* convolution modules that include a CRF decoder. However, results for the other models are more varied and depend on the base. Finally, we compared changes in AUC and PhredQ scores: in correlation to match rate, we see a mean improvement in performance in AUC when using a CRF decoder of 3%. However, we see that the CRF decoder has a harder time distinguishing correct from incorrect predictions based on the PhredQ score, with a median increase in overlap between the distributions of 30%. We concluded that using a CRF decoder is vastly superior to a CTC decoder as it improves performance almost across all metrics.

Complex convolutions are most robust, but simple convolutions are still very competitive Another main architectural difference is the complexity and depth of the convolutional layers, ranging from two or three simple convolutional layers in *Bonito*, *CATCaller* and *SACall* to more elaborate convolutional modules like *Causalcall*, *URNano* or *Mincall*. We find that the top four ranked models use the *URNano* or *Causalcall* architecture (Figure 3a). However, the six following models all use a simple CNN. Our results show that more complex convolutional architectures in general perform better, specificaally *Causalcall* and *URNano* (Figure 3c, Supplementary Figure 7). Simple convolutional architectures can also perform as good or even better than their more complex counterparts, however they are dependent on the encoder architecture that follows.

RNNs are superior to transformers, and are depth dependent Transformer layers have been gained popularity in other fields due to increased performance and speed [29]. However, our top ten models all use RNN (LSTM) layers in their encoders. A direct comparison shows that RNNs outperform Transformer layers in all the metrics (Figure 3d, Supplementary Figure 8). We also evaluated whether using deeper LSTM layers has any effect on the performance of the models. We see that there is a clear correlation between depth and performance, encouraging the use of deeper encoders for this task, regardless of the preceding convolutional architecture (Figure 3e, Supplementary Figure 9).

Training on multiple species boosts model performance across all models To assess adaptation of the model to the training dataset, in particular to the species from which the training reads originated, we evaluated the top ten models (ranked based on their performance on the human task) on the global task, which contains training and testing data from human, viral and multiple bacterial species. We observe that training on multiple species boosts the performance of all ten models across all metrics (Figure 4a). In particular, we observe a mean 3.2% improvement on match rate and mean 1.1% and 1.3% decrease in insertion and deletion rates respectively (Figure 4b). We also see a general improvement in homopolymer error rates, with decreases of 3.4% (A), 1.5% (C), 2% (G) and 4.2% (T) in mean error rate (Figure 4c). As expected, there is also an improvement in AUCs of 2.9% (Figure 6D). Surprisingly, we observe a significant decrease in the overlap between correct and incorrect base distribution, which was 35% for the human task trained models, and decreased to 21% for the global task trained models (Figure 4c). These results suggest that training on multiple species is likely to improve model generalizability, as it yields better performance across all metrics and models.

Lacking a species in the training data penalizes model performance The cross-species benchmark task is aimed at evaluating the robustness of the models to data from species they have not been trained on. We find that all models performed similarly on all bacterial species, regardless of whether they were present in the training set or not, and regardless of their k-mer genomics distance to the genomic training set (Figure 4d). However, all models perform significantly worse to the most distant reads (Homo sapiens or Lambda phage). This trend can be seen across all evaluation metrics (Supplementary Figure 10). We therefore asked whether this drop in performance, for the most difficult reads, was due to the lack of training data on those species or whether those particular species are more difficult to basecall. To answer this question, we analyzed the data from the global task in the same manner. We observed that, in general, models trained on the global task perform better (0.1%, 0.3%, 0.8%, 0.7% and 0.9% average mean match rate improvement for each bin). There is however, a similar trend in which Homo sapiens and Lambda phage data have a significantly lower performance than the rest of species. We concluded that, while these might be more difficult reads in general, the lack of training data on the cross-species task contributed to the lower performance. There are two models (*URNano-BonitoFwd* and *CATCaller-BonitoFwd*) which show the smallest differences in performance between the two tasks. These two models are also the ones that perform best overall, showcasing that their architectures are more robust to training data biases and have a better ability to generalize to unseen genomic sequences. While it may seem that the BonitoFwd LSTM encoder is the reason for their performance, we see that another model, *Bonito-BonitoFwd* does not

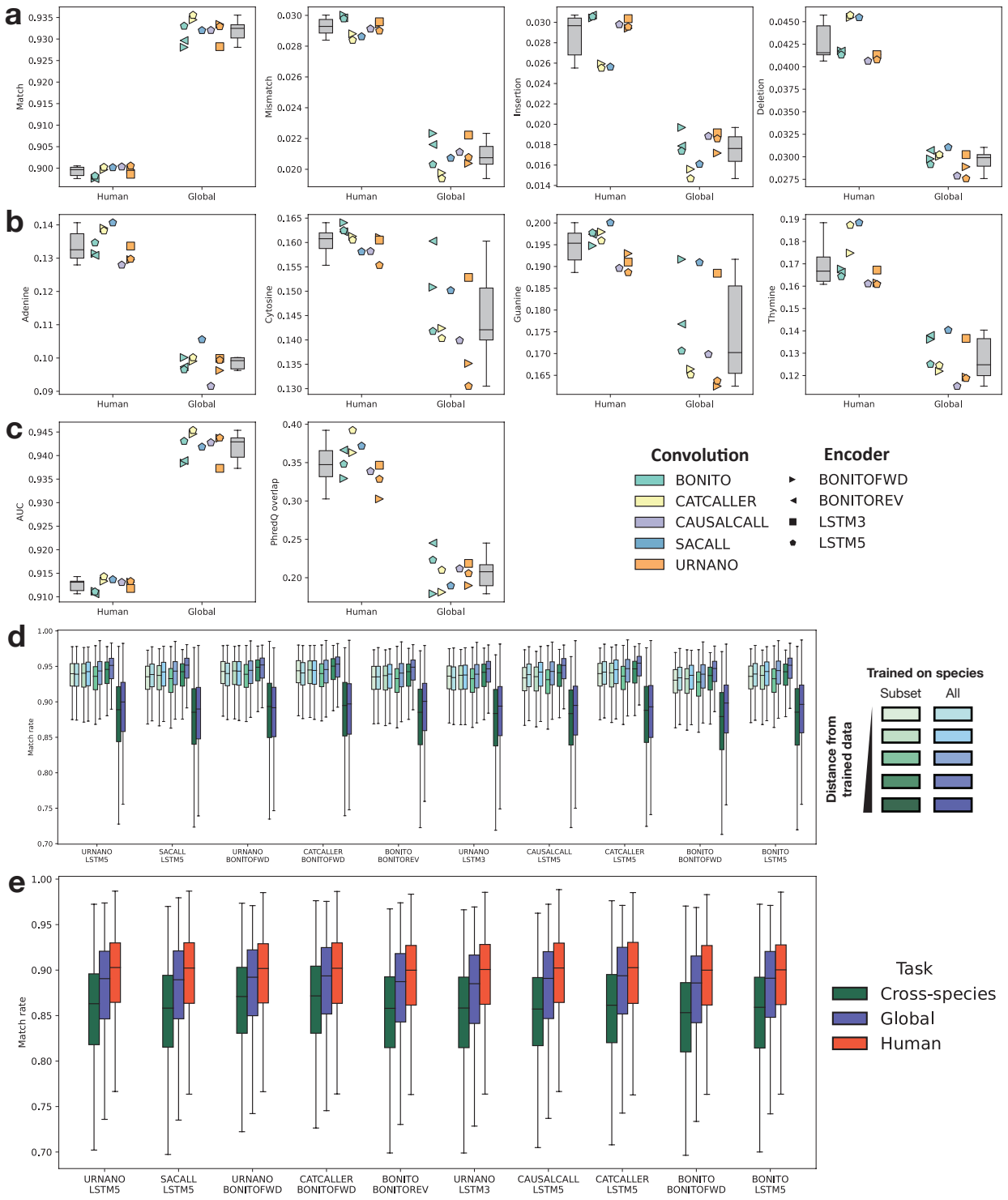

Figure 4: Performance comparison on different tasks. Comparison between the human and global task on the top 10 best performing model combinations : **(a)** Alignment event rates, **(b)** homopolymer error rates and **(c)** PhredQ scoring. **(d)** Comparison between the cross-species and global task. **(e)** Comparison between the human, global and cross-species task only on human data.

perform as well despite having the same encoder. There are three other models that also share the same convolutional modules (*URNano-LSTM5*, *URNano-LSTM3* and *CATCaller-LSTM5*) that also perform slightly worse. We conclude that it is the combination of both convolution and encoder that are necessary to achieve the best performance. Finally, we compared the performance of these models only on the Homo sapiens data and included the results from the Human task. The results again show that the lack of data is detrimental to the performance of the model (Figure 4e, Supplementary Figure 11). Furthermore, we can observe that all models performed best when only trained with Homo sapiens data, with an average mean match rate improvement of 3.8% and 1.1% when compared to the cross-species and global tasks respectively. This result might encourage the use of species specific models, however, caution should be taken as it is possible that models start to overfit and memorize the genomic sequences.

3 Discussion

Nanopore basecalling is a critical task in accurate DNA sequencing requiring complex deep learning algorithms. New algorithms for this are regularly proposed, but the lack of consensus in benchmarking data and evaluation metrics makes it complicated and cumbersome to value new contributions by the field. This problem will only grow larger as time passes and new AI technologies are used to develop even more sophisticated basecallers. To tackle this problem, we here have proposed a series of tasks (datasets for training and testing; encompassing previously used benchmarking datasets) and a set of clearly defined evaluation metrics. Our proposal is meant to serve as a starting point for what should become a community effort: both by researchers and ONT. For example, additional tasks could be added: like additional species specific datasets or small/large datasets to evaluate the required amounts of training data required by the models. Furthermore, the repertoire of evaluation metrics could be expanded [30].

Given these proposed tasks and metrics, we benchmarked the latest existing basecallers to evaluate the neural network architectures. To do so, we implemented previously published methods in a coherent framework enabling training on the same data and making a fair comparison not influenced by implementation details or platform. *Bonito* achieved the best overall performance, however, our results show that other models can obtain better results in other metrics. For this reason, it is important to keep expanding the list of metrics so that end users can choose the best model for their end goals. To further investigate the architectures of these basecallers, we created new models by combining their different components. We show that using a CRF decoder, over the more traditional CTC decoder, boosts performance significantly and it is likely the reason why Bonito performs so well in the initial benchmark. A CRF decoder predicts bases in a conditional manner, which seems to be a desirable feature given that the measured electric signal is affected by more than one base. This feature is not present in a CTC decoder which has been its main criticism over the years. We also show that deep RNNs (LSTM) are superior to Transformer layers, and that both simplex and complex convolutional architectures can achieve competitive performance. Finally, we demonstrate that species-wise, the lack of training data can decrease model performance. And species-specific tasks, models trained solely on that particular species have the potential to perform better than more general use models, however, further research and validation still has to be done on that regard to ensure that no overfitting takes place and that downstream analysis are not negatively affected.

4 Methodology

4.1 Data

We gathered datasets that had previously been used for benchmarking, were available and were sequenced using a R9.4 or R9.4.1 pore chemistry (Supplementary Table 4). With that criteria, we used the bacterial dataset from Wick et al. (2019) and the human genome reference (NA12878/GM12878, Ceph/Utah pedigree) dataset from Jain et al. (2018). The human dataset contained many different sequencing runs. We arbitrarily chose three experiments so that each different ligation kit (rapid, ligation and ultra) would be included: FAB42828, FAF09968 and FAF04090. We also included a Lambda phage dataset that we sequenced. The Lambda phage genome DNA material was purchased from NEB (N3011S). The sample was prepared according to the ONT LIgation KIT and sequenced with a MinION flow cell.

Data annotation Data was annotated using the tombo resquiggle tool (v1.5.1). First, reads were aligned to the reference sequences using their basecalls. Reference genomes were used as reference sequences for all the datasets; with the exception of the train portion of the bacterial dataset from Wick et al., (2019), which was provided already with a reference sequence for each read. Using tombo, we aligned the raw signal to the expected signal according to the reference. Reads that did not align to the reference genome or provided a bad resquiggle quality according to tombo were discarded (Supplementary Figure 1).

Tasks set splits We defined a set of reads to be used for training and testing for each task (Supplementary Table 1). For the global task, reads were split according to their mapping to their reference genome. Bacterial and lambda phage reads that mapped to the first 50% of the genome were used for training, and the rest were used for testing. Reads that mapped to both halves of the genome were discarded. Human reads that mapped odd numbered chromosomes were used for training and reads that mapped to even numbers were used for testing. A total of 100k reads were requested for training and 50k reads for testing. The number of reads was equally split for each species, therefore each species would contribute with a maximum of 3571 for training and 1785 for testing. Some species did not have sufficient reads to reach such a quota. A total of 81955 reads were used for training and 47088 reads for testing. For the human task, reads were split as described in the global challenge. For this challenge, reads were also split equally between chromosomes, and a total of 42812 and 25000 reads were used for training and testing. For the cross-species task, species were split between training and testing. For each bacterial species, we calculated the distribution of 9-mers in their reference genomes and calculated the pairwise Jensen-Shannon divergence between all species pairs. We then performed single-linkage clustering on the distance matrix and binned the distances into 4 bins (Supplementary Figure 12). We then sequentially selected species for training. Each time we selected one species, we recalculated how many species were in each bin relative to the species in the training set. We pseudo-randomly selected species that would change the distribution of the number of species per bin the least and that it would not set any bin to zero species. We continued this process until at least 10 species were chosen for training, with a maximum of 12 allowed. Testing species were divided into different difficulty categories based on their distance to the closest species in the train set (Supplementary Table 5). Similarly to the global task, a total of 50k and 25k reads were requested for training and testing. The testing set was further subdivided between 20k reads, that would come from the test species, and 5k reads, that would come from the train species. Each set of reads was equally divided between the different species. A total of 48013 reads were used for training, 5000 reads were used for testing from the training species, and 24335 reads were used for testing from the testing species.

4.2 Models

Model architectures were recreated using Pytorch (v1.9.0) based on their description in their publications and their github repositories. If their implementation was done using Pytorch, code was reused as much as possible (Supplementary Figure 13-Supplementary Figure 27).

Model training Non-recurrent models (all except *Halcyon*) were trained for 5 epochs with a batch size of 64. All models were trained on the same task data which was also given as input in the same order. Reads were sliced in non-overlapping chunks of 2000 data points. Models were trained using an Adam optimizer (initial learning rate = $1e^{-}3$, β_1 = 0.9, β_2 = 0.999, weight decay = 0). Learning rate was initially increased linearly for 5000 training steps from 0 to the initial learning rate of the optimizer as a warm-up; the learning rate was then decreased using a cosine function until the last training step to a minimum of $1e^{-}5$. To improve model stability gradients were clipped between -2 and 2. Halcyon trained similarly to non-recurrent models with the following differences: models were trained first for 1 epoch with non-overlapping chunks of 400 data points, then for 2 epochs with chunks of 1000 data points and finally for 2 epochs with chunks of 2000 data points. This was necessary because training directly using 2000 data points chunks led to unstable model training, this phenomenon is also described in the original Halcyon publication [21]. Therefore this transfer learning approach was used. Recurrent models were also trained without warm-up and with a 0.75 scheduled sampling. During training, 5% of the training data was used for validation from which accuracy and loss were calculated without gradients. Validation data was the same for all models. The state of the model was saved every 20000 training steps. The model state was chosen based on the best validation accuracy during training. Models were evaluated on hold out test data from the task being evaluated.

Original model recreation and benchmark *URNano* used cross-entropy as their loss, however, since the objective of the benchmark was basecalling and not signal segmentation, we used a CTC decoder instead. When evaluating the original *Halcyon*, we were unable to completely basecall all 25k reads in the test set due to memory limitations, we therefore compared our recreation based only on the 13k reads that were basecalled by the original *Halcyon* model from the human task test set. We used *Guppy* (v5.0.11) for the comparison between original models and our PyTorch implementations.

Architecture analysis Most models contain a convolutional module that later directly feeds into an encoder (recurrent/transformer) module. To be able to combine modules from different models without changing the original number of channels, we included a linear layer in between the convolution and encoder modules to up-scale or down-scale the number of channels. After this additional linear layer, we applied the last activation function of the preceding convolutional module. Contrary to the other models, the convolution modules from *URNano* and *Causalcall* do not reduce the amount of input timepoints. For those modules, we also included an extra convolution layer with the same

configuration as the last convolution layer in Bonito (kernel size = 19, stride = 5, padding = 9). This layer had the same number of channels as the last convolutional layer of *URNano* or *Causalcall*. This convolution layer was necessary in order to both use transformer encoders and/or a CRF decoder due to memory requirements. We also included three non-used encoder architectures: either one, three or five RNN-LSTM bidirectional stacked layers with 256 channels each.

4.3 Evaluation metrics

Evaluation metrics are based on the alignment between the predicted sequence and the reference sequence. Alignment is done using minimap2 (2.21) [31] with the ONT configuration for all metrics except accuracy. Accuracy is based on the Needleman-Wunsch global alignment algorithm implemented in parasail (1.2.4) [32]. The global alignment is configured with a match score of 2, a mismatch penalty of 1, a gap opening penalty of 8 and a gap extension penalty of 4. Accuracy is used to evaluate the best performing state of the models during training based on the validation fraction of the data. During training, short sequences have to be aligned, however, during testing, complete reads have to be aligned, for which minimap2 is necessary.

Accuracy Accuracy is defined as the number of matched bases in the alignment divided by the total number of bases in the reference sequence.

Alignment rates Match, mismatch, insertion and deletion rates are calculated as the number of events of each case divided by the length of the reference unless otherwise stated.

Homopolymer error rates Homopolymer regions are defined as consecutive sequences of the same base of length 5 or longer. Error rates on homopolymer regions are calculated by counting the number of homopolymers with errors (one or more mismatches, insertions or deletions) and dividing it by the number of homopolymers.

PhredQ scoring PhredQ scores are calculated using the fast_ctc_decode library from ONT. Average quality scores are calculated for all the correct and incorrect bases for each read. Differences between mean scores between correct and incorrect bases are reported. AUCs are calculated by sorting the basecalled reads according to their mean phred quality score and calculating the average match rate for cumulative fraction of reads in steps of 50.

Error profiles Error profiles are calculated for all 3-mers by counting the number of events (mismatches for each base, insertions and deletions) in the context of the two neighboring bases of the event itself according to the basecalls. Rates for each event are calculated by dividing each event count by the total number of 3-mer occurrences in the read. Error profiles are also calculated for each base, independently of their context. Randomness of error is defined as the Jensen-Shannon divergence between each 3-mer error profile and their corresponding base error profile.

5 Acknowledgements

We thank Tobias Dansen for critical reading of the manuscript. We thank Carlo Vermeulen for critical reading of the manuscript and donation of the Lambda phage sequencing data.

References

[1] Karen H. Miga, Sergey Koren, Arang Rhie, Mitchell R. Vollger, Ariel Gershman, Andrey Bzikadze, Shelise Brooks, Edmund Howe, David Porubsky, Glennis A. Logsdon, Valerie A. Schneider, Tamara Potapova, Jonathan Wood, William Chow, Joel Armstrong, Jeanne Fredrickson, Evgenia Pak, Kristof Tigyi, Milinn Kremitzki, Christopher Markovic, Valerie Maduro, Amalia Dutra, Gerard G. Bouffard, Alexander M. Chang, Nancy F. Hansen, Amy B. Wilfert, Françoise Thibaud-Nissen, Anthony D. Schmitt, Jon Matthew Belton, Siddarth Selvaraj, Megan Y. Dennis, Daniela C. Soto, Ruta Sahasrabudhe, Gulhan Kaya, Josh Quick, Nicholas J. Loman, Nadine Holmes, Matthew Loose, Urvashi Surti, Rosa ana Risques, Tina A. Graves Lindsay, Robert Fulton, Ira Hall, Benedict Paten, Kerstin Howe, Winston Timp, Alice Young, James C. Mullikin, Pavel A. Pevzner, Jennifer L. Gerton, Beth A. Sullivan, Evan E. Eichler, and Adam M. Phillippy. Telomere-to-telomere assembly of a complete human X chromosome. *Nature*, 585(7823):79–84, sep 2020.

[2] Mircea Cretu Stancu, Markus J Van Roosmalen, Ivo Renkens, Marleen M Nieboer, Sjors Middelkamp, Joep De Ligt, Giulia Pregno, Daniela Giachino, Giorgia Mandrile, Jose Espejo Valle-Inclan, Jerome Korzelius, Ewart De Bruijn, Edwin Cuppen, Michael E Talkowski, Tobias Marschall, Jeroen De Ridder, and Wigard P

Kloosterman. Mapping and phasing of structural variation in patient genomes using nanopore sequencing. *Nature Communications*, 8(1), 2017.

[3] John E Gorzynski, Sneha D Goenka, Kishwar Shafin, Tanner D Jensen, Dianna G Fisk, Megan E Grove, Elizabeth Spiteri, Trevor Pesout, Jean Monlong, Gunjan Baid, Jonathan A Bernstein, Scott Ceresnak, Pi-Chuan Chang, Jeffrey W Christle, Henry Chubb, Karen P Dalton, Kyla Dunn, Daniel R Garalde, Joseph Guillory, Joshua W Knowles, Alexey Kolesnikov, Michael Ma, Tia Moscarello, Maria Nattestad, Marco Perez, Maura R Z Ruzhnikov, Mehrzad Samadi, Ankit Setia, Chris Wright, Courtney J Wusthoff, Katherine Xiong, Tong Zhu, Miten Jain, Fritz J Sedlazeck, Andrew Carroll, Benedict Paten, and Euan A Ashley. Ultrarapid Nanopore Genome Sequencing in a Critical Care Setting. *New England Journal of Medicine*, 386(7):700–702, jan 2022.

[4] Arthur C Rand, Miten Jain, Jordan M Eizenga, Audrey Musselman-Brown, Hugh E Olsen, Mark Akeson, and Benedict Paten. Mapping DNA methylation with high-throughput nanopore sequencing. *Nature Methods*, 14(4):411–413, 2017.

[5] Franka J Rang, Wigard P Kloosterman, and Jeroen de Ridder. From squiggle to basepair: computational approaches for improving nanopore sequencing read accuracy. *Genome Biology*, 19(1):90, jul 2018.

[6] Yunhao Wang, Yue Zhao, Audrey Bollas, Yuru Wang, and Kin Fai Au. Nanopore sequencing technology, bioinformatics and applications. *Nature Biotechnology*, 39(11):1348–1365, 2021.

[7] Vladimír Boža, Broňa Brejová, and Tomáš Vinař. DeepNano: Deep recurrent neural networks for base calling in MinION nanopore reads. *PLOS ONE*, 12(6):e0178751, may 2017.

[8] Marcus Stoiber and James Brown. BasecRAWller: Streaming Nanopore Basecalling Directly from Raw Signal. *bioRxiv*, 2017.

[9] Haotian Teng, Minh Duc Cao, Michael B. Hall, Tania Duarte, Sheng Wang, and Lachlan J.M. M Coin. Chiron: translating nanopore raw signal directly into nucleotide sequence using deep learning. *GigaScience*, 7(5), may 2018.

[10] Alex Graves, Santiago Fernández, Faustino Gomez, and Jürgen Schmidhuber. Connectionist temporal classification: Labelling unsegmented sequence data with recurrent neural networks. In *Proceedings of the 23rd international conference on Machine learning - ICML '06*, pages 369–376, New York, New York, USA, jun 2006. ACM Press.

[11] Neven Miculinić, Marko Ratković, and Mile Šikić. MinCall - MinION end2end convolutional deep learning basecaller. *GitHub*, apr 2019.

[12] Kaiming He, Xiangyu Zhang, Shaoqing Ren, and Jian Sun. Deep residual learning for image recognition. *Proceedings of the IEEE Computer Society Conference on Computer Vision and Pattern Recognition*, December:770–778, 2016.

[13] Jingwen Zeng, Hongmin Cai, Hong Peng, Haiyan Wang, Yue Zhang, and Tatsuya Akutsu. Causalcall: Nanopore Basecalling Using a Temporal Convolutional Network. *Frontiers in Genetics*, 10:1332, jan 2020.

[14] Aaron van den Oord, Sander Dieleman, Heiga Zen, Karen Simonyan, Oriol Vinyals, Alex Graves, Nal Kalchbrenner, Andrew Senior, and Koray Kavukcuoglu. WaveNet: A Generative Model for Raw Audio. *arXiv e-prints*, pages 1–15, 2016.

[15] Neng Huang, Fan Nie, Peng Ni, Feng Luo, and Jianxin Wang. SACall: a neural network basecaller for Oxford Nanopore sequencing data based on self-attention mechanism. *IEEE/ACM Transactions on Computational Biology and Bioinformatics*, XX(X):1–10, 2020.

[16] Xuan Lv, Zhiguang Chen, Yutong Lu, and Yuedong Yang. An End-to-end Oxford Nanopore Basecaller Using Convolution-augmented Transformer. *IEEE/ACM Transactions on Computational Biology and Bioinformatics*, page 6, 2020.

[17] Ashish Vaswani, Noam Shazeer, Niki Parmar, Jakob Uszkoreit, Llion Jones, Aidan N. Gomez, Łukasz Kaiser, and Illia Polosukhin. Attention is all you need. *Advances in Neural Information Processing Systems*, 2017-Decem(Nips):5999–6009, 2017.

[18] Zhanghao Wu, Zhijian Liu, Ji Lin, Yujun Lin, and Song Han. Lite Transformer with Long-Short Range Attention. *ICLR 2020*, pages 1–13, 2020.

[19] Yao-Zhong Zhang, Arda Akdemir, Georg Tremmel, Seiya Imoto, Satoru Miyano, Tetsuo Shibuya, and Rui Yamaguchi. Nanopore basecalling from a perspective of instance segmentation. *BMC Bioinformatics*, 21(136), 2020.

[20] Olaf Ronneberger, Philipp Fischer, and Thomas Brox. *U-Net: Convolutional Networks for Biomedical Image Segmentation*, pages 234–241. Springer International Publishing, Cham, 2015.

[21] Hiroki Konishi, Rui Yamaguchi, Kiyoshi Yamaguchi, Yoichi Furukawa, and Seiya Imoto. Halcyon: An accurate basecaller exploiting an encoder-decoder model with monotonic attention. *Bioinformatics*, 37(9):1211–1217, jun 2021.

[22] Ilya Sutskever, Oriol Vinyals, and Quoc V. Le. Sequence to sequence learning with neural networks. *Advances in Neural Information Processing Systems*, 4(January):3104–3112, 2014.

[23] Minh Thang Luong, Hieu Pham, and Christopher D. Manning. Effective approaches to attention-based neural machine translation. *Conference Proceedings - EMNLP 2015: Conference on Empirical Methods in Natural Language Processing*, pages 1412–1421, 2015.

[24] John Lafferty, Andrew McCallum, and Fernando C.N. Pereira. Conditional Random Fields: Probabilistic Models for Segmenting and Labeling Sequence Data. *Deparmental papers (CIS), University of Pennsylvania*, 11(1):1–84, 2001.

[25] John Moult, Fidelis Krzystof, Andriy Kryshtafovych, Torsten Schwede, and Anna Tramontano. Critical assessment of methods of protein structure prediction (CASP) — round x. *Proteins*, 82(02):1–6, 2014.

[26] Alexander Sczyrba, Peter Hofmann, Peter Belmann, David Koslicki, Stefan Janssen, Johannes Dröge, Ivan Gregor, Stephan Majda, Jessika Fiedler, Eik Dahms, Andreas Bremges, Adrian Fritz, Ruben Garrido-Oter, Tue Sparholt Jørgensen, Nicole Shapiro, Philip D. Blood, Alexey Gurevich, Yang Bai, Dmitrij Turaev, Matthew Z. Demaere, Rayan Chikhi, Niranjan Nagarajan, Christopher Quince, Fernando Meyer, Monika Balvočiutė, Lars Hestbjerg Hansen, Søren J. Sørensen, Burton K.H. Chia, Bertrand Denis, Jeff L. Froula, Zhong Wang, Robert Egan, Dongwan Don Kang, Jeffrey J. Cook, Charles Deltel, Michael Beckstette, Claire Lemaitre, Pierre Peterlongo, Guillaume Rizk, Dominique Lavenier, Yu Wei Wu, Steven W. Singer, Chirag Jain, Marc Strous, Heiner Klingenberg, Peter Meinicke, Michael D. Barton, Thomas Lingner, Hsin Hung Lin, Yu Chieh Liao, Genivaldo Gueiros Z. Silva, Daniel A. Cuevas, Robert A. Edwards, Surya Saha, Vitor C. Piro, Bernhard Y. Renard, Mihai Pop, Hans Peter Klenk, Markus Göker, Nikos C. Kyrpides, Tanja Woyke, Julia A. Vorholt, Paul Schulze-Lefert, Edward M. Rubin, Aaron E. Darling, Thomas Rattei, and Alice C. McHardy. Critical Assessment of Metagenome Interpretation - A benchmark of metagenomics software. *Nature Methods*, 14(11):1063–1071, 2017.

[27] Going for algorithm gold, 2008.

[28] Ludmil B Alexandrov, Serena Nik-Zainal, David C Wedge, Peter J Campbell, and Michael R Stratton. Deciphering Signatures of Mutational Processes Operative in Human Cancer. *Cell Reports*, 3(1):246–259, jan 2013.

[29] Shigeki Karita, Nanxin Chen, Tomoki Hayashi, Takaaki Hori, Hirofumi Inaguma, Ziyan Jiang, Masao Someki, Nelson Enrique Yalta Soplin, Ryuichi Yamamoto, Xiaofei Wang, Shinji Watanabe, Takenori Yoshimura, and Wangyou Zhang. A comparative study on transformer vs rnn in speech applications. *ASRU 2019*, 2019.

[30] Clara Delahaye and Jacques Nicolas. Sequencing dna with nanopores: Troubles and biases. *PLOS ONE*, 16(10):1–29, 10 2021.

[31] Heng Li. Minimap2: pairwise alignment for nucleotide sequences. *Bioinformatics*, 34(18):3094–3100, 05 2018.

[32] Jeff Daily. Parasail: SIMD c library for global, semi-global, and local pairwise sequence alignments. *BMC Bioinformatics*, 17(1), February 2016.

[33] Ryan R. Wick, Louise M. Judd, and Kathryn E. Holt. Performance of neural network basecalling tools for Oxford Nanopore sequencing. *Genome Biology*, 20(1):1–10, jun 2019.

[34] Miten Jain, Sergey Koren, Karen H Miga, Josh Quick, Arthur C Rand, Thomas A Sasani, John R Tyson, Andrew D Beggs, Alexander T Dilthey, Ian T Fiddes, Sunir Malla, Hannah Marriott, Tom Nieto, Justin O'Grady, Hugh E Olsen, Brent S Pedersen, Arang Rhie, Hollian Richardson, Aaron R Quinlan, Terrance P Snutch, Louise Tee, Benedict Paten, Adam M Phillippy, Jared T Simpson, Nicholas J Loman, and Matthew Loose. Nanopore sequencing and assembly of a human genome with ultra-long reads. *Nature Biotechnology*, 36(4):338–345, January 2018.

[35] Nick Loman. Data, 2016.